Tribology International 182 (2023) 108354

Contents lists available at ScienceDirect

Tribology International

journal homepage: www.elsevier.com/locate/triboint

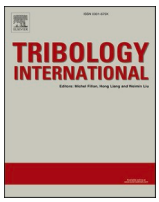

Multi-objective optimization of tool wear, surface roughness, and material removal rate in finishing honing processes using adaptive neural fuzzy inference systems

Irene Buj-Corral [a,*], Piotr Sender [a,b], Carmelo J. Luis-Pérez [c]

[a] Department of Mechanical Engineering, Barcelona School of Industrial Engineering (ETSEIB), Universitat Politècnica de Catalunya-Barcelona Tech (UPC), 08028 Barcelona, Spain

[b] Institute of Manufacturing and Materials Technology, Faculty of Mechanical Engineering and Ship Technology, Gdańsk University of Technology, ul. Narutowicza 11/12, 80-233 Gdańsk, Poland

[c] Engineering Department. Public University of Navarre (UPNA), Arrosadia Campus, 31006 Pamplona, Spain

ARTICLE INFO

Keywords:
Roughness
Cylindricity
Tool wear
Material removal rate
Honing
ANFIS
Modeling

ABSTRACT

Honing processes are usually employed to manufacture combustion engine cylinders and hydraulic cylinders. Honing provides a crosshatch pattern that favors the oil flow. In this paper, Adaptive Neural Fuzzy Inference System (ANFIS) models were obtained for tool wear, average roughness Ra, cylindricity and material removal rate in finishing honing processes. In addition, multi-objective optimization with the desirability function method was applied, in order to determine the process parameters that allow minimizing roughness, cylindricity error and tool wear, while maximizing material removal rate. The results showed that grain size and tangential velocity should be at their minimum levels, while density, pressure and linear velocity should be at their maximum levels. If only roughness, cylindricity error and tool wear are considered, then low grain size, low pressure and low linear velocity are recommended, while density and tangential velocity vary, depending on the optimization algorithm employed. This work will help to select appropriate process parameters in finishing honing processes, when roughness, cylindricity error and tool wear are to be minimized.

1. Introduction

Honing processes are commonly employed in finishing operations of internal cylinders of combustion engines and of hydraulic cylinders [1]. In this process, a honing head is used, which is provided with abrasive stones. The combination of a reciprocating linear movement and a rotation movement provides a crosshatch pattern with oil channels [2]. These channels have a profound effect on the tribological performance of the equipment, because they can be used to retain oil or grease to ensure proper lubrication and minimize wear of the different components [3].

In the past, several authors have studied roughness and material removal rate in honing processes. As a general trend, roughness increases with grain size [4,5]. It is also important to choose a tool with proper density, because this will influence both surface roughness and the level of wear of the abrasive stone [6]. Pressure is known to decrease roughness [7]. As described by Tripathi et al. [8], other factors influencing roughness are honing speed and machining time. As for productivity, Kadyrov [9] found that the honing efficiency depends on the pressure of the honing stone against the part, the honing time, the cylinder shape deviation and the roughness value of the surface. Mezghani et al. [10] observed that greater material loss is observed for higher number of strokes. Vrac et al. [11] observed that, when using D181 abrasive stones, machining speed had the greatest impact on the honing performance, while when using D151 pressure was most influential factor. The same authors found a correlation between surface roughness and material removal rate [4]. They reported specific material removal rate values up to 0.02016 mm/s (0.12 cm/min). On the other hand, Szabo [12] found greater material removal rate for cBN stones than for Al_2O_3 ones. Another work showed that material removal rate is directly related totangential speed and linear speed, but it increases to a greater extent when both speeds take high values [12].

However, there is less information on tool wear and cylindricity error in honing processes. For instance, Cabanettes et al. [13] found a

* Corresponding author.
E-mail addresses: irene.buj@upc.edu (I. Buj-Corral), piosend1@pg.edu.pl (P. Sender), cluis.perez@unavarra.es (C.J. Luis-Pérez).

https://doi.org/10.1016/j.triboint.2023.108354
Received 28 October 2022; Received in revised form 19 January 2023; Accepted 16 February 2023
Available online 21 February 2023

Table 1
Levels of the input variables.

Input Variables			Low	Center	High
GS:	Grain Size	(ISO 6106[32])	15	20	30
DE:	Density	(ISO 6104[33])	10	15	20
PR:	Pressure	(N/cm^2)	400	500	600
TV:	Tangential Speed	(m/min)	20	30	40
LV:	Linear Speed	(m/min)	20	30	40

Table 2
Output variables.

Ra:	Average roughness	(μm)
Cil_t:	Total cylindricity	(μm)
Qp:	Tool wear	(cm^3/min)
Qm:	Material removal rate	(cm/min)

Fig. 1. Honing test machine from Honingtec S.A.

Fig. 2. St-52 steel cylinders.

correlation between surface roughness of cylinder liners and tool wear in motor blocks. Specifically, areal roughness parameters Spk (reduced peak height) and Ssc (arithmetic mean summit curvature) have a high correlation with wear. As for cylindricity, Zhang et al. [14] developed a methodology to reduce this kind or form error in engine cylinder bores.

Fig. 3. cBN abrasive stones with metallic bond.

It consists of simulating the motion trajectory, improving the structure of the head, coordinating the honing operation with the previous boring operation and optimizing the honing parameters. Xi et al. [15] found that the stroke length is an important factor influencing cylindricity of the inner hole, as well as the honing pressure. On the other hand, El Mansori et al. found that low acceleration values in the stroke movement reduce the cylindricity error [16].

Fuzzy Inference Systems (FIS) and Adaptive Neural Fuzzy Inference System (ANFIS) have been widely employed for modelling manufacturing processes variables, where Takagi-Sugeno [17] and Mamdani [18,19] are the most used [20]. A large amount of research studies dealing with the application of soft computing and design of experiments can be found in the literature where hybrid learning procedures that combine artificial neural networks (ANNs) and fuzzy inference systems (FIS) stand out. From the initial research study of Jang [21], several studies using ANFIS have been developed, as shown in Shihabudheen and Pillai [22].

In regard with tool wear, material removal rate and roughness, several studies can be found where neural networks as well as FIS and ANFIS are combined with design of experiments in order to model these output variables [23]. For example, in the research study of Marani et al. [24] an ANFIS was employed for modeling the flank wear in the turning process of a cold-finished steel bar. In another study Abbas et al. [25] analyzed the influence of depth of cut, cutting length, feed rate, and cutting speed on surface roughness, flank wear, power consumption and material removal rate (MRR) in the high-speed turning of Ti-6Al-4V. A fuzzy comprehensive evaluation model was developed in Li et al. [26] in order to evaluate the tribological properties of friction materials. In Sudheer et al. [27] ANFIS and neural networks combined with design of experiments were employed to predict surface roughness and metal removal rate in grinding process where the input parameters analyzed were speed, depth of cut and feed rate. Further examples are the study of Feng et al. [28], who studied the Rk-family roughness parameters and that of Buj et al. [29], who analyzed the application of an adaptive neural network to predict average roughness Ra in honing processes. In addition, Sharma et al. [30] employed ANN and a Taguchi Design of Experiments (DOE), and Vališ et al. [31] carried out an analysis of oil contaminants by using a fuzzy inference system (FIS) and multilayer perceptron neural networks.

The main aim of this present study is to analyze the effect of Grain size (GS), Density (DE), Pressure (PR) and both Tangential speed (TV) and Linear speed (LV) on surface fnish, tool wear, material removal rate and form error in finishing honing processes by using adaptive neural

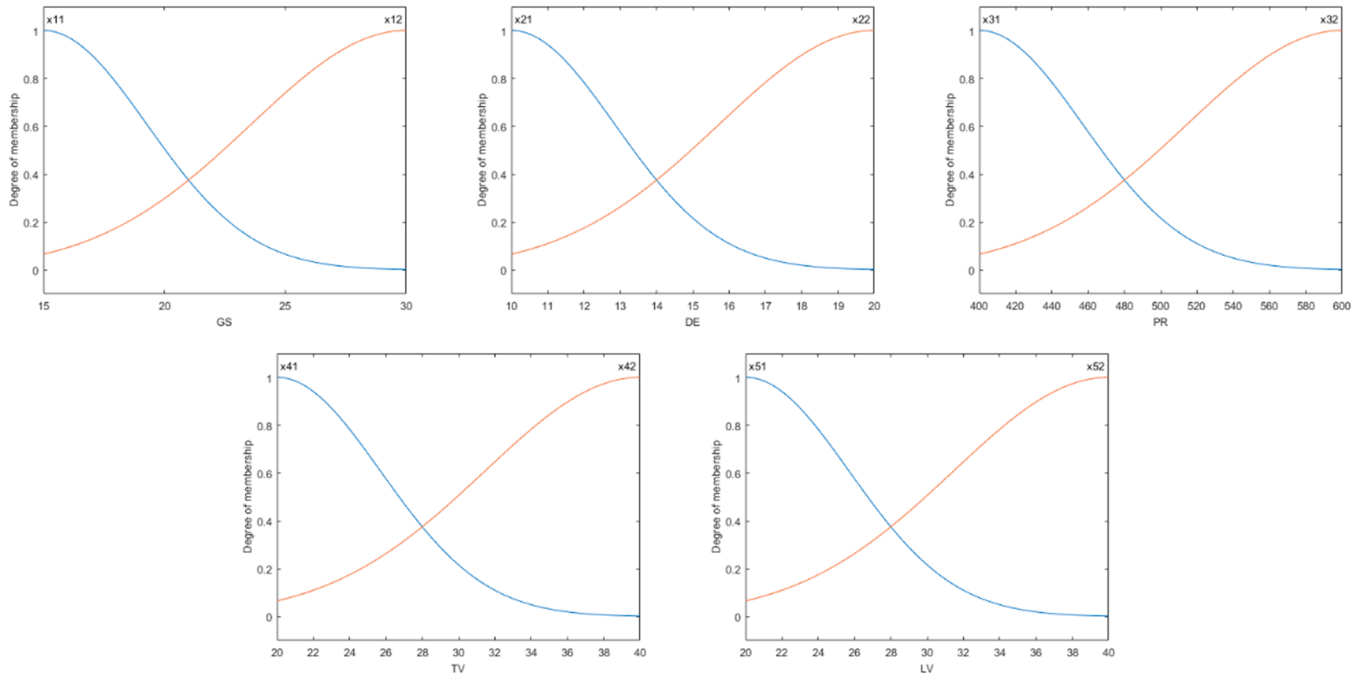

Fig. 4. Membership functions for fuzzification of the inputs.

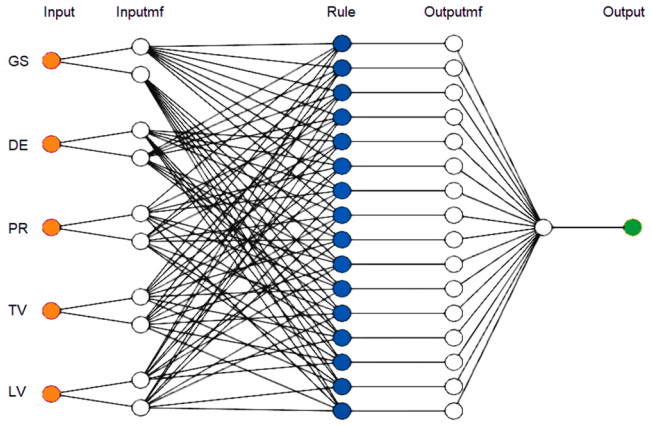

Fig. 5. Schematics of the ANFIS model for Qm.

fuzzy inference systems and a multi-optimization process from the previously obtained models. The output variables to be analyzed are: average roughness Ra (μm), tool wear, Qp (cm^3/min) and material removal rate Qm (cm/min) Likewise, cylindricity error, Cilt (μm) is also studied. In addition, multi-objective optimization is carried out by means of the desirability function, in order to minimize roughness, cylindricity error and tool wear, while maximizing material removal rate.

2. Materials and methods

The experiments were defined according to a fractional factorial design 2^{5-1} with two levels of the variables and three center points as shown in Table 1 and Table 2.

The levels of the different variables correspond to the final honing phase or finishing honing phase, in which the final surface texture is obtained. This phase is usually carried out after the rough and the semi-finishing phases. For example, grain size between 91 and 181 is commonly employed in rough honing, grain size between 46 and 64 in semi-finishing honing, and grain size below 46 is used in semi-finishing operations. As for density, it is directly related to grain size, i.e., lower grain size requires lower density as a general trend. In this case, density values between 10 and 20 were recommended. Pressure values are limited to 1000 N/cm^2 in the machine that was used in the present work (Section 2.1). Finally, in this work the same ranges for tangential and linear speed were chosen, between 20 and 40 m/min. Due to the design of the machine, it is advisable to use linear speed values of 40 m/min or lower, while tangential speed could take higher values.

2.1. Set-up of the honing experiments

A test honing machine from Honingtec S.A. was used (Fig. 1). Unlike usual industrial machines, it has a horizontal configuration, and the rotation movement is provided by the rotation of the part, not of the honing head.

St-52 steel cylinders were used of 50 mm in internal diameter and 150 mm in length (Fig. 2).

Cubic boron nitride (cBN) stones were employed of 3 × 3×20 mm (Fig. 3). The honing head has three abrasive stones.

The stones were fixed to the tool holder with glue, and the tool holders were mechanically fixed to the honing head.

2.2. Surface roughness measurements

Surface roughness was measured in a Taylor Hobson Talysurf 2 roughness meter. A Gaussian filter was employed with a cut-off value of 0.8 mm and a measuring length of 4.8 mm. Three measurements were carried out along generatrices of the internal surface of the cylinders, which were separated 120°. The area where the measurements were performed is approximately in the middle of the part, in order to avoid both ends of the cylinder, corresponding to acceleration/deceleration of the honing head.

Average roughness parameter Ra was considered, which is commonly employed in industry to compare different machined surfaces.

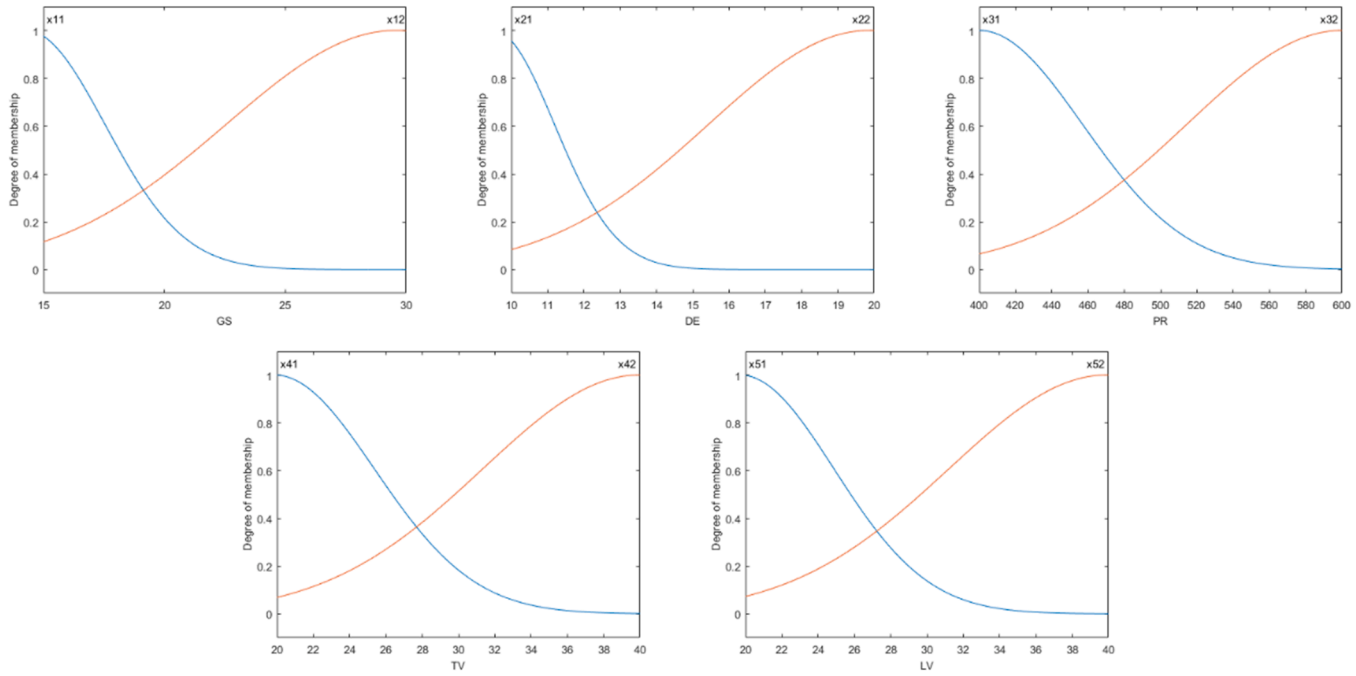

Fig. 6. Membership functions after the ANFIS for modelling Qm.

Table 3
Results of the honing tests.

Run	GS	DE	PR (N/cm^2)	TV (m/min)	LV (m/min)	Ra (μm)	Cylt (μm)	Qp (cm^3/min)	Qm (cm/min)
1	15	20	400	20	20	0.07	10.19	0.004	0.016
2	15	20	600	40	20	0.10	27.30	0.003	0.062
3	15	20	600	20	40	0.05	19.46	0.002	0.131
4	15	20	400	40	40	0.11	28.65	0.001	0.041
5	15	10	600	20	20	0.10	21.70	0.002	0.015
6	15	10	400	40	20	0.08	26.89	0.001	0.007
7	15	10	400	20	40	0.09	26.56	0.002	0.015
8	15	10	600	40	40	0.09	25.15	0.003	0.025
9	30	20	600	20	20	0.51	71.70	0.009	0.221
10	30	20	400	40	20	0.20	15.93	0.003	0.111
11	30	20	400	20	40	0.34	81.45	0.007	0.163
12	30	20	600	40	40	0.57	76.90	0.016	0.301
13	30	10	400	20	20	0.26	19.52	0.004	0.059
14	30	10	600	40	20	0.54	20.51	0.004	0.048
15	30	10	600	20	40	0.53	22.41	0.003	0.053
16	30	10	400	40	40	0.24	17.20	0.004	0.080
17	20	15	500	30	30	0.18	26.65	0.019	0.182
18	20	15	500	30	30	0.25	23.91	0.014	0.220
19	20	15	500	30	30	0.25	19.80	0.018	0.211

2.3. Cylindricity measurements

Total cylindricity of the internal surface of the cylinders was measured in a Taylor Hobson Talyrond roundness measurement machine. Roundness was measured on 4 different planes at different heights of the part. From the 4 different circumferences, the cylindricity error was determined.

2.4. Tool wear and material removal rate measurements

Tool wear Qp was determined from the measurement of the initial and final height of the abrasive stones by means of a Mitutoyo digital dial indicator.

Material removal rate Qm was calculated from the initial and final diameter of the cylinders, which was measured with a Mitutoyo internal dial indicator.

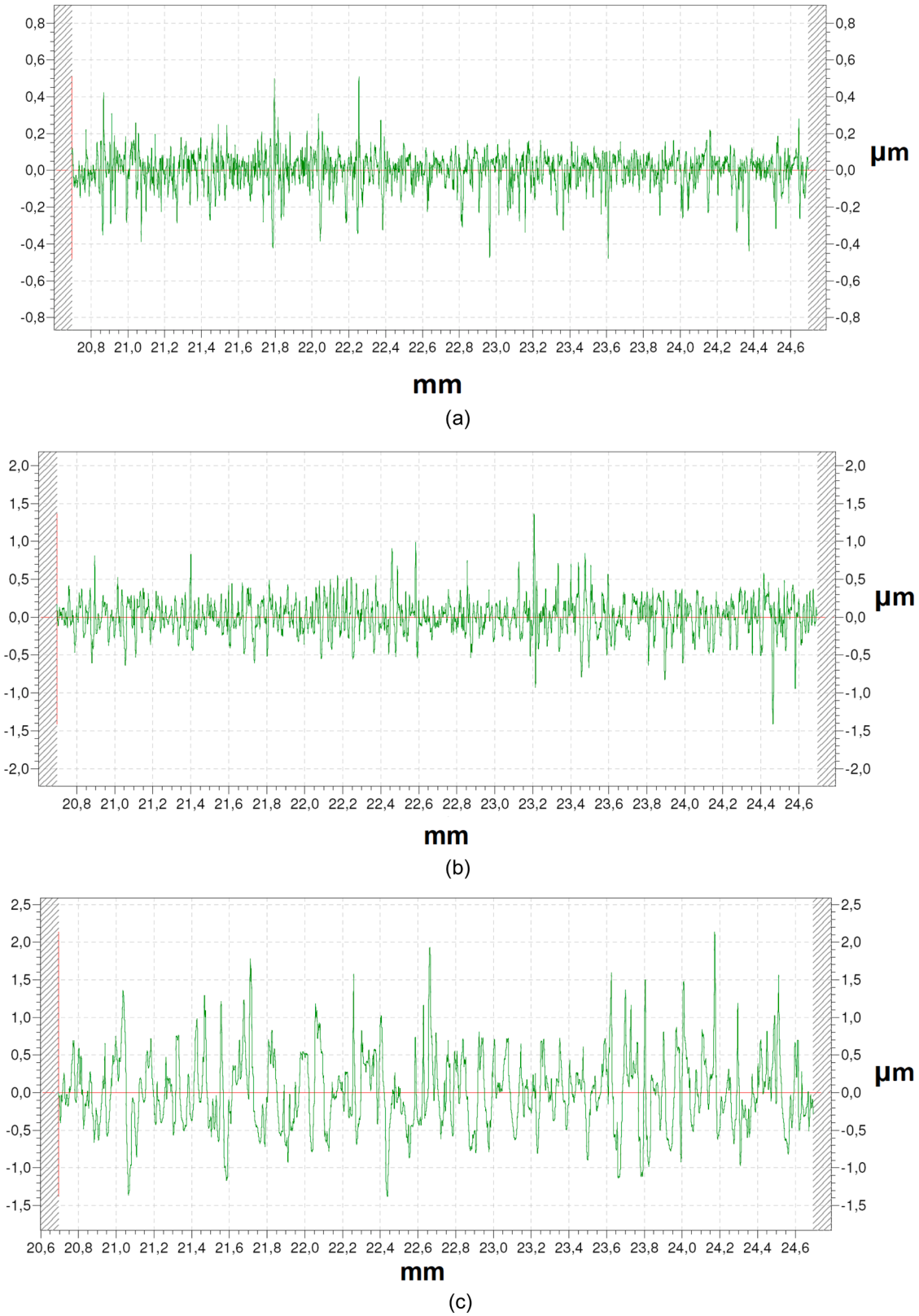

Fig. 7. Examples of roughness profiles for: a) grain size 15, b) grain size 20, c) grain size 30.

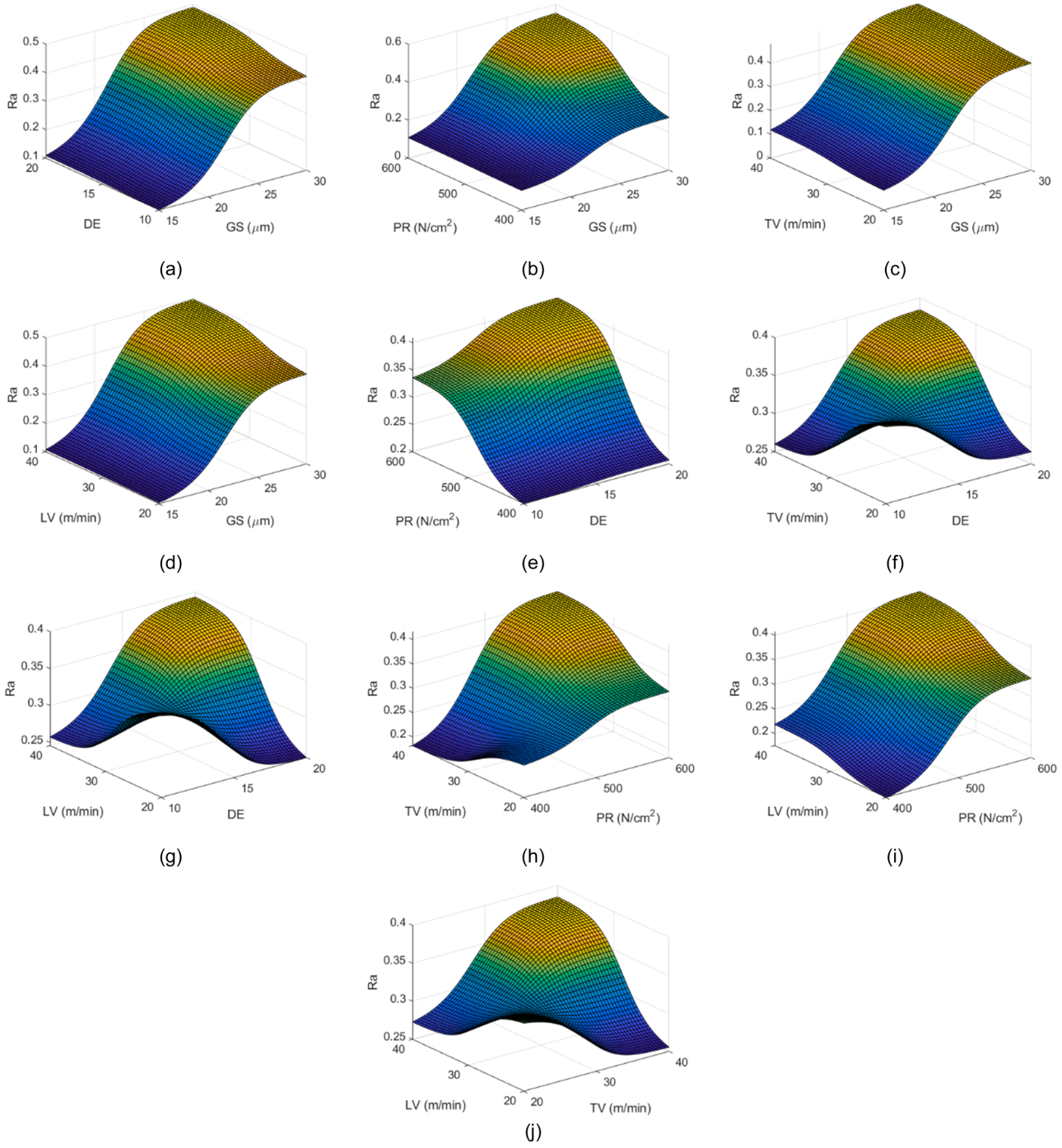

Fig. 8. Response surface for Ra (μm) versus each pair of input variables while the rest are kept at their central values, using the ANFIS developed for Ra: a) DE vs GS, b) PR vs GS, c) TV vs GS, d) LV vs GS, e) PR vs DE, f) TV vs DE, g) LV vs DE, h) TV vs PR, i) LV vs PR, j) LV vs TV.

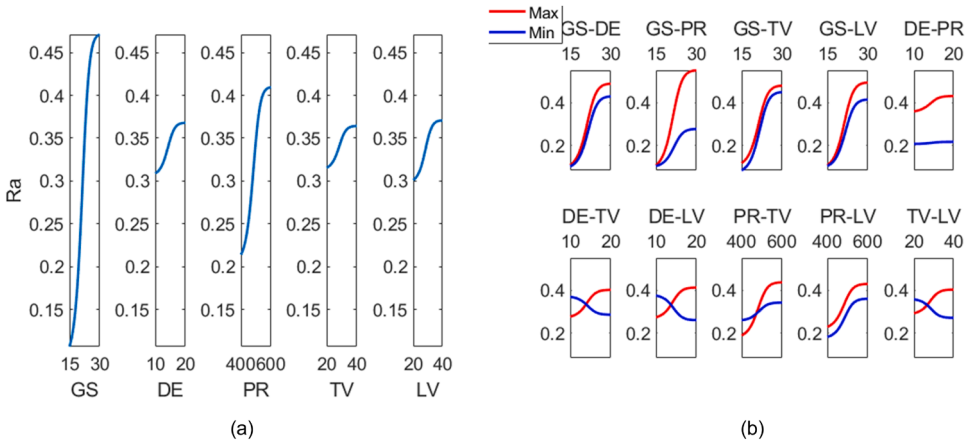

Fig. 9. (a) Main effects plot and (b) interaction effects plot for Ra (μm).

2.5. ANFIS modeling

A zero-order Sugeno FIS was developed by using the Fuzzy Logic Toolbox™ of Matlab™2020a [34]. This FIS was employed because the de-fuzzification process is computationally more efficient compared to that of a Mamdani system [34–36]. As can be observed in Fig. 4 the membership functions employed in this study are of the Gaussian type, as shown in Eq. (1), where two membership functions were employed for each of the input variables shown in Table 1.

$$\mu_x = e^{\frac{-(x-c)^2}{2\sigma^2}} \tag{1}$$

In the Sugeno FIS developed for each of the outputs, the aggregation method employed is the sum of fuzzy sets, and the aggregated output is obtained from the weighted average of all output rules. Eq. (2) shows the implication method and Eq. (3) shows the output of the Sugeno system [34–37].

$$w_j(x) = AndMethod\{\mu_1(x_1), \ldots, \mu_n(x_n)\} \tag{2}$$

$$output_j = \frac{\sum_{j=1}^{Numberofrules} w_j * z_j}{\sum_{j=1}^{Numberofrules} w_j} \tag{3}$$

As previously mentioned, zero-order Sugeno FISs were developed for each of the output variables. Where output corresponds to Ra, Cylindricity, Qp and Qm. Each of the FISs have a set of n rules of the form shown by Eq. (4):

$$if\ \left((x_1\ is\ x_{1,i1})\ and\ (x_2\ is\ x_{2,i2})\ and\ \ldots\ and\ (x_5\ is\ x_{5,i5})\right)\ then\ output_j\ is\ z_j \tag{4}$$

Once the initial Sugeno FIS were developed, then an ANFIS was employed to tune the parameters of the membership functions using the Fuzzy Logic Toolbox™ of Matlab™2020a [34]. Finally, these tuned FIS were employed for modeling the behavior of the output variables shown in Table 2. Fig. 5 shows the schematics of the ANFIS model for Qm. A similar scheme is employed, for the rest of outputs.

Fig. 6 shows the membership functions after the ANFIS for the case of Qm.

2.6. Multi-objective optimization

In order to carry out a multi-objective optimization of the outputs, a desirability function can be employed. In this study two desirability functions are considered: the one proposed by Luis-Perez [38] and the one proposed by Derringer&Suich [39]. As is known, the desirability function transforms a multi-variable optimization problem into a one-dimensional optimization problem [39].

The main objective of this present study is to minimize the surface roughness, which is characterized by the average surface roughness (Ra (μm)), because it is one of the most used parameters in the industry, although, any other roughness parameter could have been used. Likewise, a shape parameter is also minimized, which in this study is the total cylindricity (μm). In addition, two important parameters with opposite behavior have been considered in the present optimization. The first one is tool wear (Qp (cm^3/min)) and the material removal rate (Qm (cm/min)), so that tool wear should be minimized, and material removal rate should be maximized.

$$D = (f_{t1} * f_{t2} * f_{t3} * f_{t4})^{\frac{1}{4}} \tag{5}$$

Although other means could be used such as the harmonic one, in this present study the geometric mean will be used, as Eq. (5) shows, where f_j is the variable transformed using the desirability function mentioned above.

3. Results and discussion

Table 3 contains the results for roughness (Ra), cylindricity (Cylt), material removal rate (Qm) and tool wear (Qp).

Highest Ra value of 0.57 μm corresponds to experiment 12, obtained with high grain size of 30, high density of 20, high pressure of 400 N/cm^2, high linear speed of 40 m/min and high tangential speed of 40 m/min. These conditions lead to high material removal rate of 0.301 cm/min but also to high cylindricity error of 76.90 μm and high tool wear of 0.016 cm^3/min. For these reasons, this combination is not recommended in finishing honing operations. Experiments 9 and 12 also showed high material removal rate, and experiment 2 lead to medium values of material removal rate, suggesting that the combination of high density of 20 and high pressure of 600 N/cm^2 is not appropriate in finishing honing.

As a general trend, the experiments in which low grain size was used (experiments 1–8) lead to low roughness values equal or lower than 0.11 μm. Higher grain size leads to higher roughness values of up to 0.57 μm, which are similar to those reported previously [40].

Fig. 7 corresponds to three different roughness profiles obtained with grain size 15, 20 and 30 respectively:

The three profiles in Fig. 7 are irregular, as is usual in abrasive machining processes. As expected, the higher grain size, the higher roughness is. In Fig. 7(a) (grain size 15), total roughness value Rt value is lower than 1 μm, in Fig. 7(b) (grain size 20) it is lower than 3 μm and in Fig. 7(c) (grain size 30) it is lower than 4 μm.

In the production of cylinder liners, El-Mansori et al. reported

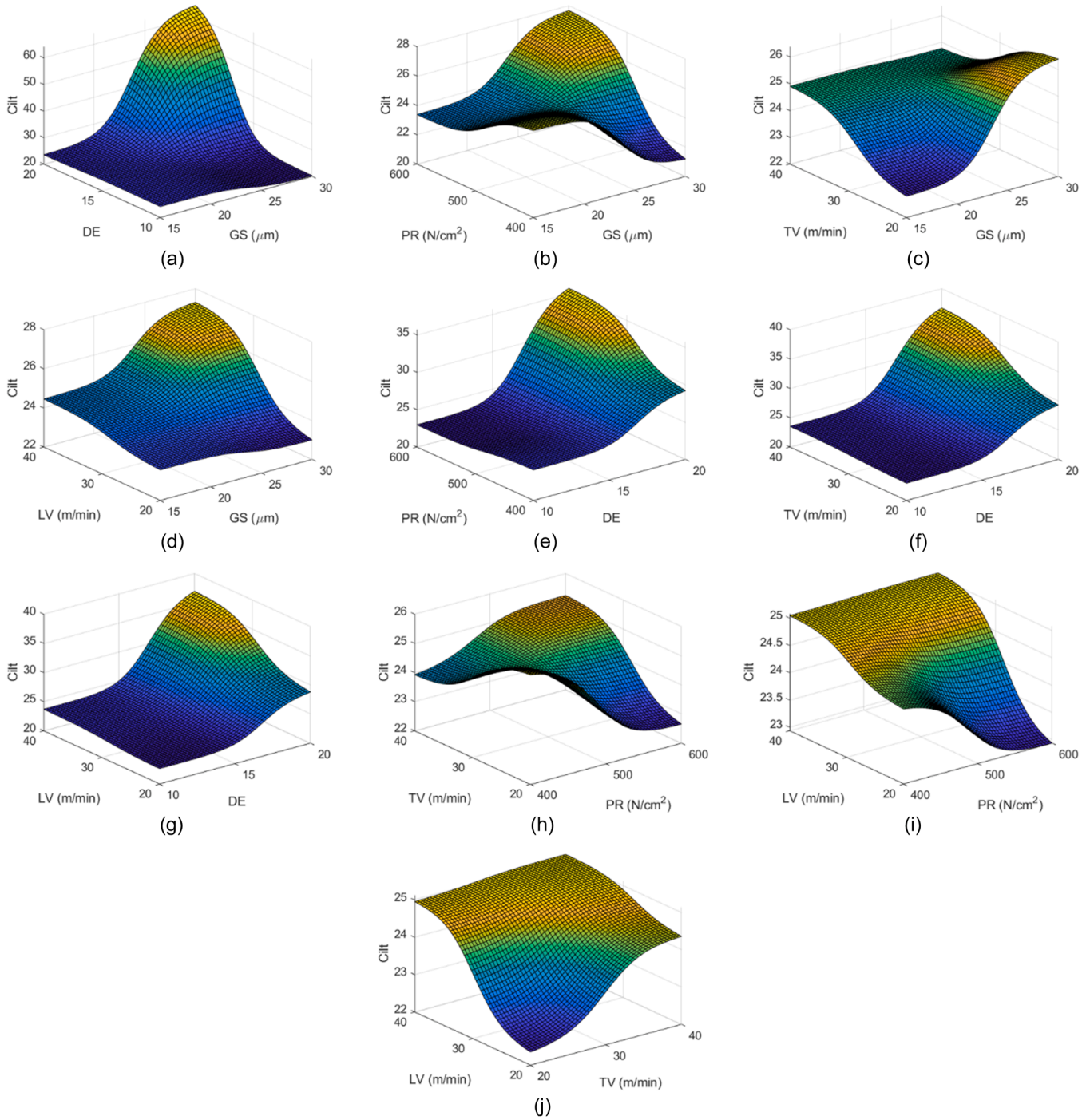

Fig. 10. Response surface for Cylindricity (μm) versus each pair of input variables while the rest are kept at their central values, using the ANFIS developed for the cylindricity: a) DE vs GS, b) PR vs GS, c) TV vs GS, d) LV vs GS, e) PR vs DE, f) TV vs DE, g) LV vs DE, h) TV vs PR, i) LV vs PR, j) LV vs TV.

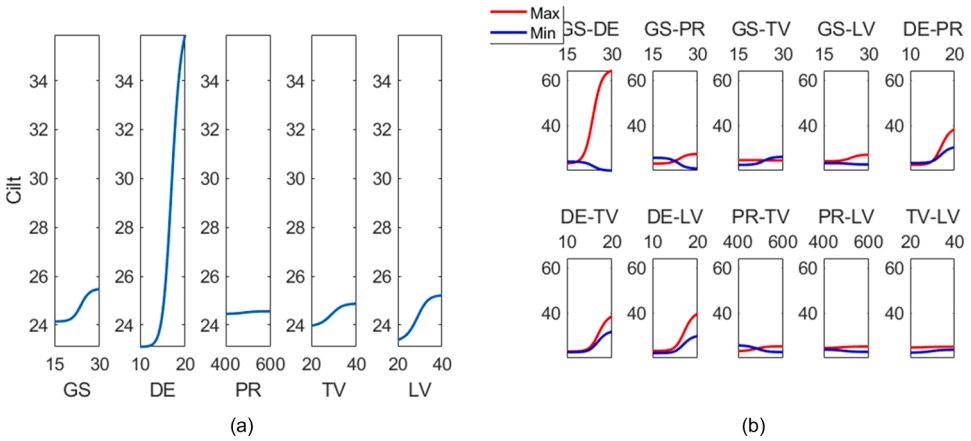

Fig. 11. (a) Main effects plot and (b) interaction effects plot for Cylindricity (μm).

cylindricity errors of up to 15.3 μm [41], which are similar to those reported in this work when low grain size is employed. On the contrary, high grain size leads to higher cylindricity error.

The use of low grain size (experiments 1–8) also led to low tool wear below 0.005 cm^3/min. Higher grain size lead to higher tool wear values of 0.019 $cm^{3/}$min. In rough honing processes with cBN (cubic boron nitride) stones, higher tool wear values of up to 0.122 cm^3/min were obtained [42].

In general, low material removal rate values were reported, except for experiment 3 with 0.131 cm/min. Similar material removal rates of 0.12 cm/min were reported by Vrac et al. [4] for diamond stones in rough honing. Buj-Corral and Sivatte-Adroer [42] reported material removal rates of more than 0.50 cm/min in rough honing with cBN stones.

3.1. Roughness

Fig. 8 depicts the response surface for the case of Ra using the ANFIS models.

Fig. 9(a) shows the main effects plot and Fig. 9(b) contains the interaction effects plots for Ra, using the ANFIS models. In the case of the main effects plot, each variable is varied within its minimum and maximum levels, while the rest of the factors are kept at their central level. In the case of the interaction effect plots one variable is set at its minimum and maximum level, respectively, and the other one is varied within the minimum and maximum values while the rest of the variables are kept at their central values. In Fig. 9(b), corresponding to the interaction between grain size and pressure, it can be observed that, in order to obtain low roughness, the combination of high grain size and high pressure should be avoided. The reason for this is that, in this case, grains will dig deeper into the material, leaving deeper marks and leading to higher average roughness values.

As can be observed in Fig. 9(a) the most influential parameter on the average surface roughness (Ra) is the grain size (GS), followed by the pressure (PR), so that the larger the grain size or pressure, the higher the Ra values obtained. Grain size and pressure are known to influence roughness in honing processes [40,43]. The same behavior is observed for the rest of the variables. Therefore, from the point of view of reducing the Ra values, all input parameters should be kept at their minimum levels, which can also be observed in the interaction plots in Fig. 9(b).

3.2. Cylindricity

Fig. 10 shows the response surface for the case of the cylindricity (Cyl_t) using the ANFIS models.

Fig. 10(a) shows the interaction between grain size and density. It can be observed that, in order to obtain low cylindricity, high density withhigh grain size should be avoided. This combination can lead to clogging in the honing stone because the chip can fill in the gaps on the stones' surface [6].

Fig. 11(a) corresponds to the main effects plots and Fig. 11(b) to the interaction plots for the cylindricity (Cylt). As can be observed in Fig. 11 (a) the most influential parameter on cylindricity is density (DE), followed by lineal velocity (LV) grain size (GS), so that the higher the density or grain size, the higher the cylindricity values obtained. The same behavior is observed for the rest of the variables. Therefore, from the point of view of reducing the cylindricity values, all input parameters should be kept at their minimum levels. This can also be observed in the interaction plots shown in Fig. 10(b). Lu et al. [44] reported lower cylindricity error when low pressure was used. The cylindricity error also depends on the stroke length.

3.3. Tool wear Qp / Material removal rate Qm

Fig. 12 shows the response surface for the case of the tool wear (Qp), using the ANFIS models.

Fig. 12 corresponds to the interaction between grain size and density. In order to minimize tool wear, low grain size and/or low density should be chosen.

Fig. 13(a) depicts to the main effects plots and Fig. 13(b) the interaction plots for tool wear (Qp).

As observed with the two previous output parameters (Ra and Cylindricity), to reduce tool wear all input parameters should be kept at their minimum levels. As can be seen in Fig. 13(a) the most influential parameter in order to reduce tool wear is grain size (GS) and density (DE), followed by linear velocity (LV), so the higher the values of these input parameters, the higher the tool wear. The same behavior is observed for the rest of the variables. Therefore, from the point of view of reducing tool wear, all input parameters should be kept at their minimum levels. This can also be seen in the interaction plots shown in Fig. 13(b).

Fig. 14 shows the response surface for the case of the material removal rate (Qm) using the ANFIS models.

Fig. 14(a), corresponding to the interaction between grain size and density, shows that, in order to obtain high material removal rate, the combination of high grain size and high density is expected, which is opposite to the recommendations to decrease cylindricity error and tool wear.

Fig. 15(a) shows to the main effects plots and Figure 13(b) the interaction plots for material removal rate (Qm).

As can be seen in Fig. 15(a) all input variables should be kept at their maximum levels, in order to obtain the highest material removal rate (Qm). As expected, this is opposite behavior to that observed for Ra,

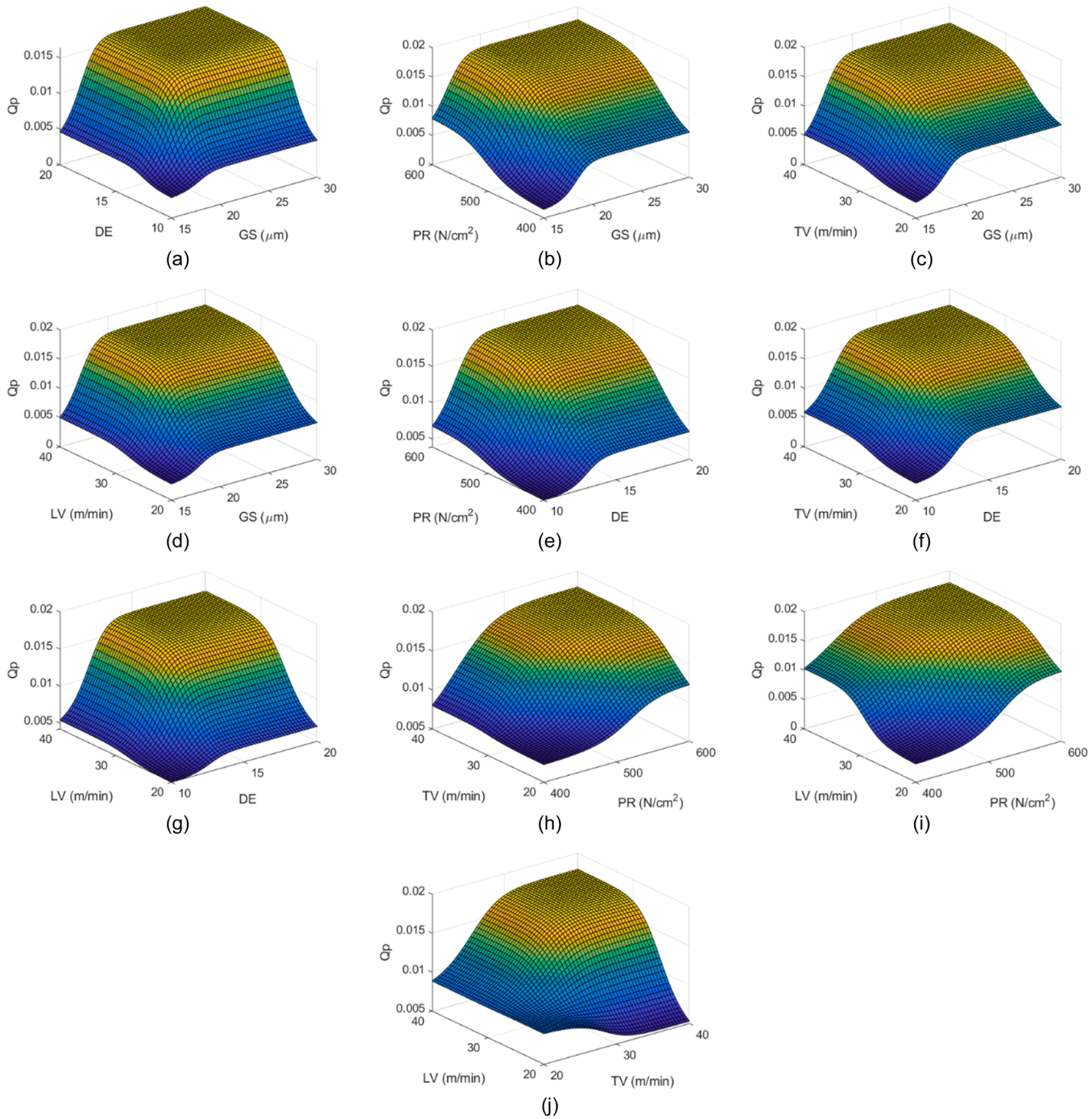

Fig. 12. Response surface for Qp (cm^3/min) versus each pair of input variables while the rest are kept at their central values, using the ANFIS developed for Qp: a) DE vs GS, b) PR vs GS, c) TV vs GS, d) LV vs GS, e) PR vs DE, f) TV vs DE, g) LV vs DE, h) TV vs PR, i) LV vs PR, j) LV vs TV.

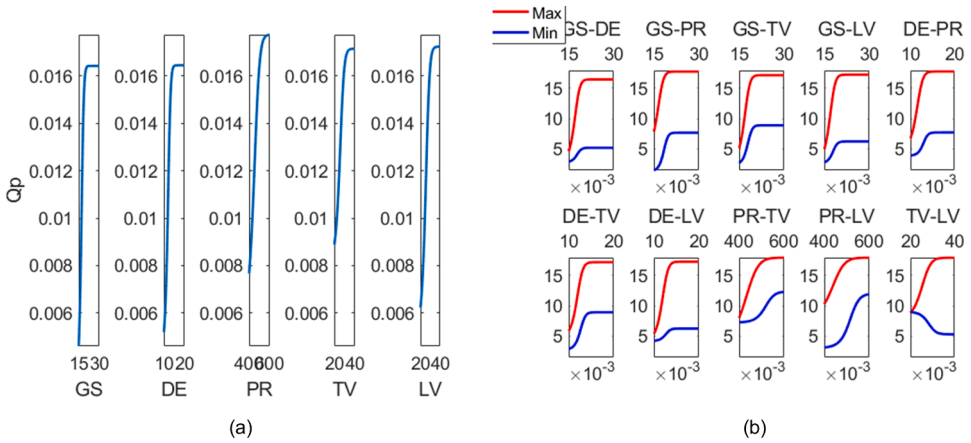

Fig. 13. (a) Main effects plot and (b) interaction effects plot for Qp (cm^3/min).

cylindricity and tool wear. The most influential parameters on the material removal rate are DE and GS, followed by PR, LV and TV, to a lesser extent.

3.4. Multi-objective optimization

In honing processes, usually roughness and material removal rate have an opposite behavior. As a general trend, in order to obtain high material removal rate, high grain size is employed, but this worsens surface finish and, in addition, increases tool wear. In this work, in a first optimization approach, the four responses were considered. Two kinds of desirability functions were employed: Luis-Pérez [38] and Derringer&Suich [39].

Fig. 16 shows the transformation employed in order to carry out the multi-objective optimization using the Luis-Pérez desirability function, where the codification is as follows: 1 Ra, 2 Cilindricity, 3 Qp and 4 Qm and "t" corresponds to the transformation employing the desirability function of Luis-Pérez [38]. In this case, more weighting was given to roughness and tool wear than to the other responses.

Likewise, Fig. 17 shows the transformation employed in order to carry out the multi-objective optimization, when the Derringer&Suich desirability function is employed, with an r factor equal to three. Similarly, the codification is as follows: 1 Ra, 2 Cilindricity, 3 Qp and 4 Qm and "d" corresponds to the transformation employing the desirability function of Derringer&Suich [39]. In this case, the same weighting value was used for all the responses analyzed, in order to compare the results obtained with both desirability functions.

The same results were found for the two different desirability functions. They are presented in Table 4.

It should be noted that the output values correspond to those predicted by the ANFIS models. However, as can be seen, the optimum value found by the multi-objective optimization corresponds to an experimental point (run number 3). Therefore, in this case, the actual values of the output variables could be used, and the optimal results would be those shown in Table 5.

Results obtained by both desirability functions suggest that the range of values of the design factors could be widened to improve the obtained results, so that both the tangential velocity and the grain size could be reduced, while density, pressure and linear velocity could be higher in another design of experiments in order to analyze if there is an optimum solution within these new range of values.

On the other hand, multi-objective optimization could lead to different values that are close to the optimum and could be selected instead. Therefore, an increment of 0.1% in relation to the optimum value is selected to find the predicted values by the multi-objective optimization. That is, the predicted values (y_j) that are within ($optimum\ value * (1 - 0.001) \leq y_j \leq optimum\ value$) are selected. These results are shown in Table 6 for the desirability function of Luis-Pérez [38] and in Table 7 for the desirability function of Derringer&Suich [39]. It should be mentioned that any other increment could have been used.

Table 6 shows the values that satisfy that the $optimum\ value * (1 - 0.001) \leq y_j \leq optimum\ value$ for the case of the Luis-Pérez desirability function [38] and Table 7 shows the values obtained for the Derringer&Suich desirability function [39]. If the increment is enlarged, more than 0.1%, other values could be found that could be of technological interest, depending on the characteristics of the finishing process.

As was observed in Table 4, the preferred values to simultaneously optimize roughness, cylindricity, tool wear and material removal rate are those where GS and TV are kept at their lowest levels, while the preferred levels for DE, PR and LV are the highest.

Since in this work finishing honing operations are considered, in which low material removal rate is expected, it may be of industrial interest to optimize surface roughness as well as cylindricity and tool wear rather than material removal rate. Therefore, a similar optimization process is carried out in a second approach. The results obtained are shown in Table 8 and in Table 9 for both desirability functions. It is worth mentioning that, depending on the transformation used, it is possible to obtain different values in the optimization using a desirability function, which justify the difference in the values obtained when using the two desirability functions considered in this present study.

In Tables 8 and 9 it can be observed that, in order to simultaneously minimize surface roughness, cylindricity error and tool wear, low grain size of 15 (ISO 6106), low pressure of 400 N/cm^2 and low linear velocity of 20 m/min are recommended. Different density and tangential velocity values should be employed depending on the desirability function that is employed. If the Derrigner&Suich function is selected (Table 8), then the combination of high density of 20 (ISO 6104) and low tangential velocity of 20 m/min is recommended. If the Luis-Pérez function is considered (Table 9), then the combination of low density of 20 (ISO 6104) and high tangential velocity of 40 m/min is recommended.

4. Conclusions

In this work experimental finishing honing tests were carried out. Average roughness Ra, cylindricity Cylt, material removal rate Qm and tool wear Qp were measured.

The combination of high grain size, high density, high pressure, high tangential speed and high linear speed is not recommended, because it provides high roughness, high cylindricity error and high tool wear.

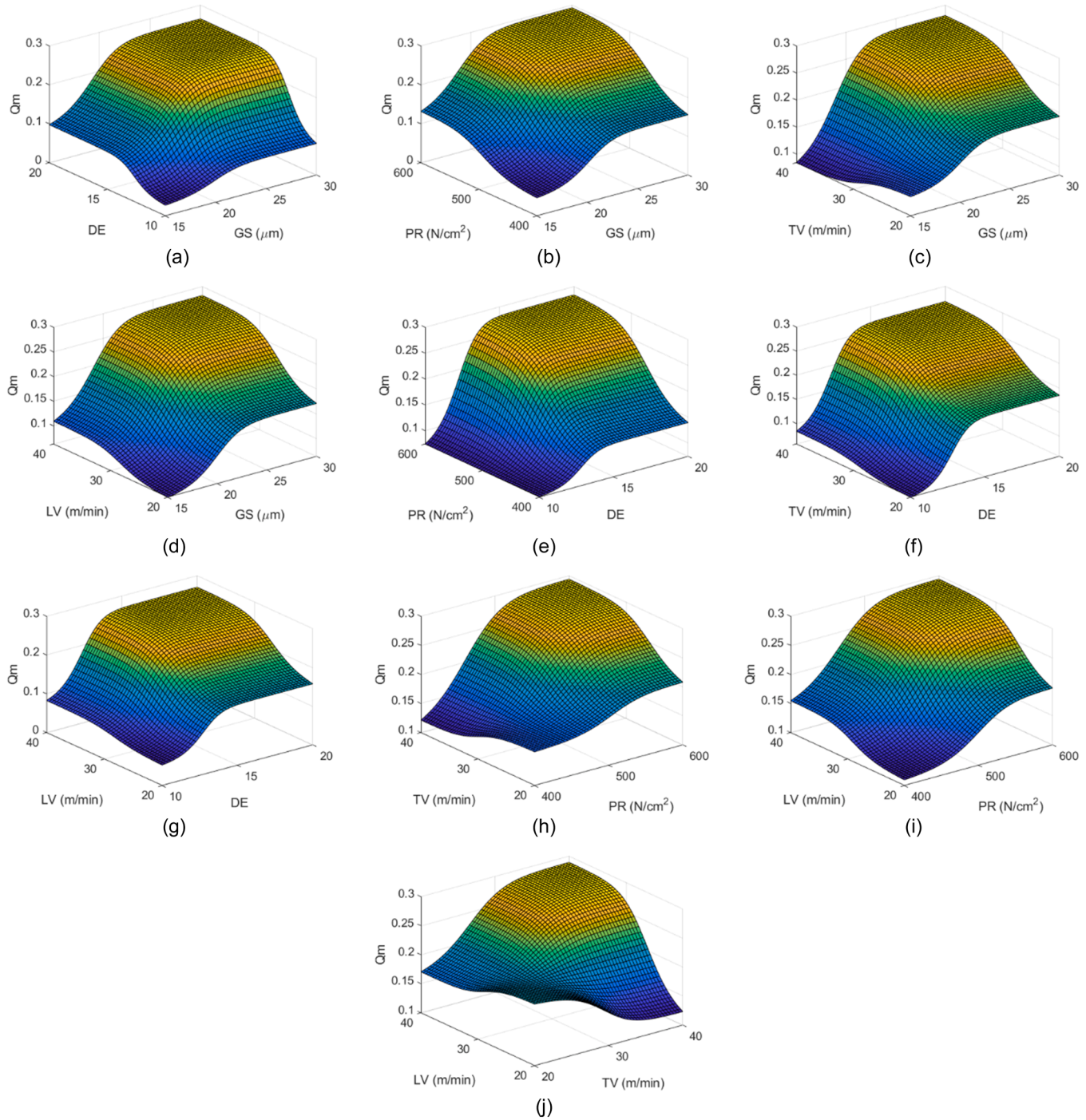

Fig. 14. Response surface for Qm (cm/min) versus each pair of input variables while the rest are kept at their central values, using the ANFIS developed for Qm: a) DE vs GS, b) PR vs GS, c) TV vs GS, d) LV vs GS, e) PR vs DE, f) TV vs DE, g) LV vs DE, h) TV vs PR, i) LV vs PR, j) LV vs TV.

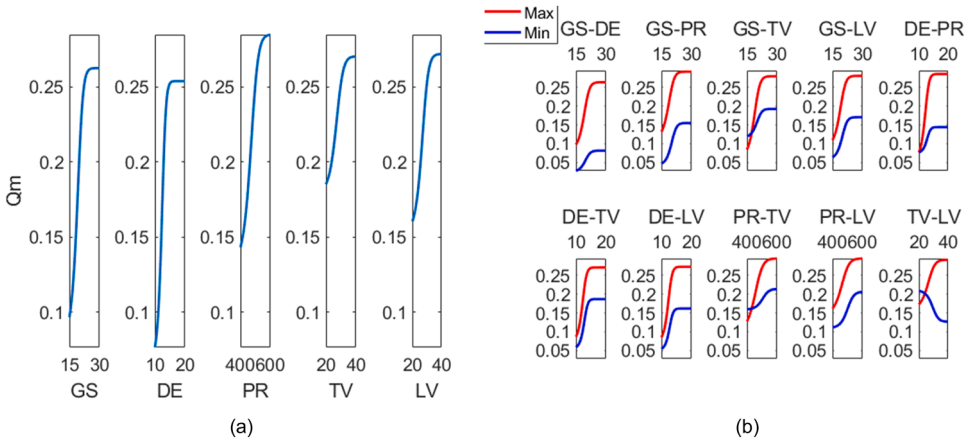

Fig. 15. (a) Main effects plot and (b) interaction effects plot for Qm (cm/min).

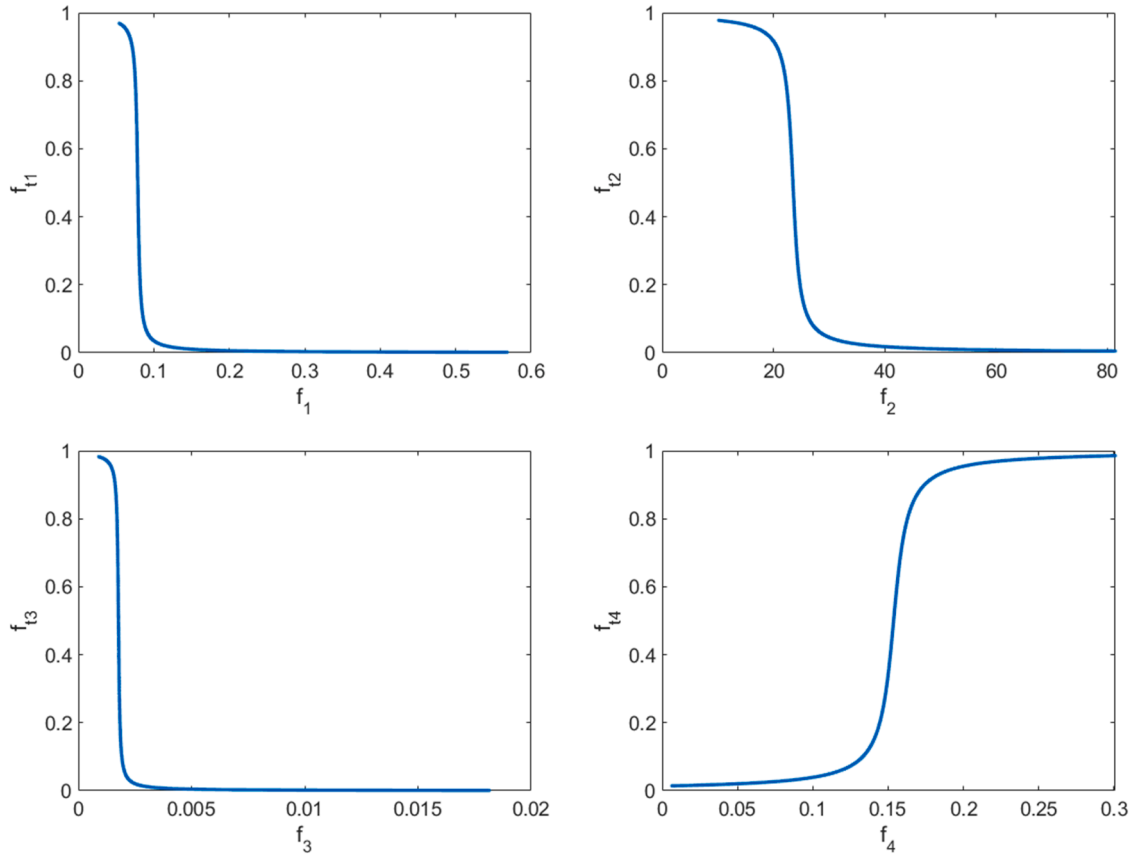

Fig. 16. Transformation of the values of the response functions obtained by using the ANFIS and the desirability function proposed by Luis-Pérez [38].

ANFIS models are presented for the studied responses. Moreover, two desirability functions are employed in order to perform a multi-objective optimization.

From the point of view of minimizing the surface roughness, as well as the cylindricity and the tool wear it has been obtained that all inputs (GS, DE, PR, LV and TV) should be kept at their minimum levels. This is an opposite behavior of that for material removal rate, where all inputs should be at their highest values.

When the objective is to minimize roughness, cylindricity and tool wear and, at the same time, increase the material removal rate, it was observed that grain size and tangential velocity should be at their minimum levels, while density, pressure and linear velocity should be at their maximum levels. Therefore, results obtained suggest that the range of values of the design factors could be widened in order to improve the obtained results, so that both tangential velocity and grain size could be reduced, while density, pressure and linear velocity could be higher, in order to analyze if there is an optimum solution within these new range of values. This could be done in a future study.

On the other hand, when the objective is to minimize tool wear, as well as roughness and cylindricity, but material removal rate is not considered, then grain size, pressure and linear velocity should be kept at their minimum levels, while the recommended value for density and tangential velocity depend on the desirability function employed. However, from the results it has been observed that, if density is kept at its maximum level and tangential velocity at its minimum level, then cylindricity improves more than tool wear and, on the other hand, if

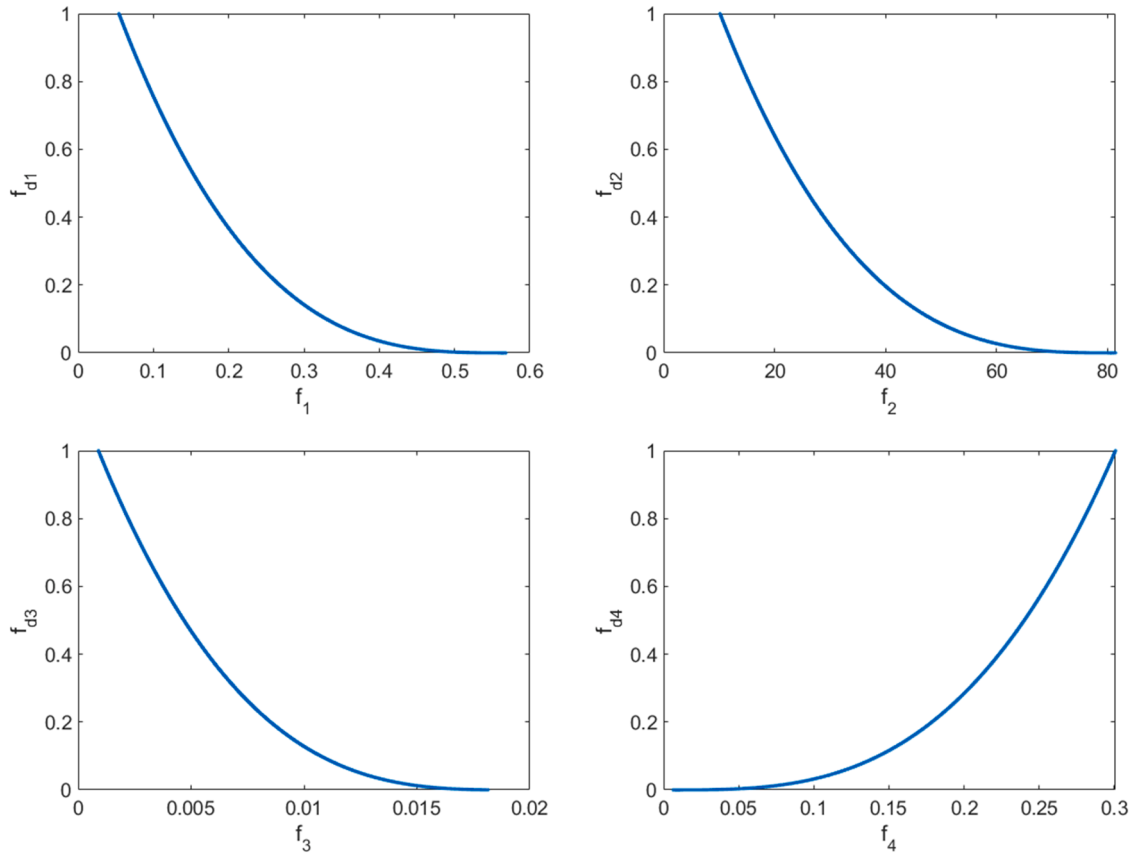

Fig. 17. Transformation of the values of the response functions obtained by using the ANFIS and the desirability function proposed by Derringer&Suich [39].

Table 4
Results of the multi-objective optimization (values predicted by the ANFIS models).

GS	DE	PR (N/cm^2)	TV (m/min)	LV (m/min)	Ra (μm)	Cylt (μm)	Qp (cm^3/min)	Qm (cm/min)
15	20	600	20	40	0.054	19.459	0.002	0.131

density is kept at its minimum level and tangential velocity at its maximum level, then tool wear improves more than cylindricity, without significant modifications of roughness in both cases.

Declaration of Competing Interest

The authors declare that they have no known competing financial interests or personal relationships that could have appeared to influence the work reported in this paper.

Table 5
Results of the multi-objective optimization (experimental values).

run	GS	DE	PR (N/cm^2)	TV (m/min)	LV (m/min)	Ra (μm)	Cylt (μm)	Qm (cm/min)	Qp (cm^3/min)
3	15	20	600	20	40	0.05	19.46	0.002	0.131

Table 6
Results (y_j) of the multi-objective optimization where ($optimum\ value * (1-0.001) \leq y_j \leq optimum\ value$) using the Luis-Pérez desirability function [38].

GS	DE	PR (N/cm^2)	TV (m/min)	LV (m/min)	Ra (μm)	Cylt (μm)	Qp (cm^3/min)	Qm (cm/min)
15.000	19.286	600.000	20.000	35.714	0.055	19.515	0.002	0.131
15.000	18.571	600.000	20.000	37.143	0.055	19.518	0.002	0.131
15.000	19.286	600.000	20.000	37.143	0.055	19.492	0.002	0.131
15.000	20.000	600.000	20.000	37.143	0.054	19.476	0.002	0.131
15.000	17.857	600.000	20.000	38.571	0.055	19.545	0.002	0.131
15.000	18.571	600.000	20.000	38.571	0.055	19.504	0.002	0.131
15.000	19.286	600.000	20.000	38.571	0.054	19.480	0.002	0.131
15.000	20.000	600.000	20.000	38.571	0.054	19.465	0.002	0.131
15.000	17.857	600.000	20.000	40.000	0.055	19.536	0.002	0.131
15.000	18.571	600.000	20.000	40.000	0.055	19.497	0.002	0.131
15.000	19.286	600.000	20.000	40.000	0.054	19.474	0.002	0.131
15.000	**20.000**	**600.000**	**20.000**	**40.000**	**0.054**	**19.459**	**0.002**	**0.131**

Table 7
Results (y_j) of the multi-objective optimization where ($optimum\ value * (1 - 0.001) \leq y_j \leq optimum\ value$) using the Derringer&Suich desirability function [39].

GS	DE	PR (N/cm^2)	TV (m/min)	LV (m/min)	Ra (μm)	Cylt (μm)	Qp (cm^3/min)	Qm (cm/min)
15.000	20.000	585.714	20.000	35.714	0.055	19.499	0.002	0.131
15.000	20.000	600.000	20.000	35.714	0.055	19.497	0.002	0.131
15.000	19.286	585.714	20.000	37.143	0.055	19.496	0.002	0.131
15.000	20.000	585.714	20.000	37.143	0.054	19.479	0.002	0.131
15.000	19.286	600.000	20.000	37.143	0.055	19.492	0.002	0.131
15.000	20.000	600.000	20.000	37.143	0.054	19.476	0.002	0.131
15.000	20.000	571.429	20.000	38.571	0.054	19.476	0.002	0.131
15.000	19.286	585.714	20.000	38.571	0.054	19.484	0.002	0.131
15.000	20.000	585.714	20.000	38.571	0.054	19.468	0.002	0.131
15.000	18.571	600.000	20.000	38.571	0.055	19.504	0.002	0.131
15.000	19.286	600.000	20.000	38.571	0.054	19.480	0.002	0.131
15.000	20.000	600.000	20.000	38.571	0.054	19.465	0.002	0.131
15.000	20.000	571.429	20.000	40.000	0.054	19.471	0.002	0.131
15.000	19.286	585.714	20.000	40.000	0.054	19.478	0.002	0.131
15.000	20.000	585.714	20.000	40.000	0.054	19.463	0.002	0.131
15.000	18.571	600.000	20.000	40.000	0.055	19.497	0.002	0.131
15.000	19.286	600.000	20.000	40.000	0.054	19.474	0.002	0.131
15.000	**20.000**	**600.000**	**20.000**	**40.000**	**0.054**	**19.459**	**0.002**	**0.131**

Table 8
Results (y_j) of the second multi-objective optimization using the Derringer&Suich desirability function [39].

GS	DE	PR (N/cm^2)	TV (m/min)	LV (m/min)	Ra (μm)	Cylt (μm)	Qp (cm^3/min)
15.000	20.000	400.000	20.000	20.000	0.0704	10.1898	0.0035

Table 9
Results (y_j) of the second multi-objective optimization using the Luis-Pérez desirability function [38].

GS	DE	PR (N/cm^2)	TV (m/min)	LV (m/min)	Ra (μm)	Cylt (μm)	Qp (cm^3/min)
15.000	10.000	400.000	40.000	20.000	0.0748	26.8894	0.0009

Data availability

Data will be made available on request.

Acknowledgements

The authors would like to thank the company Honingtec S.A. as well as Alejandro Domínguez for their help with the experimental tests. Financial support of these studies from Gdańsk University of Technology, Poland, by the DEC-6/2021/IDUB/IV.2/EUROPIUM application number 035506 grant under the IDUB - 'Excellence Initiative - Research University' program is gratefully acknowledged.

References

[1] Klocke F. Manufacturing Processes 2 - Grinding, Honing, Lapping. Springer,; 2009.
[2] Mezghani S, Demirci I, Yousfi M, El Mansori M. Mutual influence of crosshatch angle and superficial roughness of honed surfaces on friction in ring-pack tribosystem. Tribol Int 2013. https://doi.org/10.1016/j.triboint.2013.04.014.
[3] Wang Q, Feng Q, Li QF, Ren CZ. The experimental investigation of stone wear in honing. Key Eng Mater 2011;487:462–7. https://doi.org/10.4028/www.scientific.net/KEM.487.462.
[4] Vrac D., Sidjanin L., Balos S. The Effect of Honing Speed and Grain Size on Surface Roughness and Material Removal Rate during Honing. vol. 11. n.d.
[5] Blank G, Cutter R, Elhami S, Razfar MR, Farahnakian M, Rasti A, et al. Experimental study of effective parameters on honing process of cast iron cylinder. Int J Adv Manuf Technol 2012;2:1829–37.
[6] Buj-Corral I, Álvarez-Flórez J, Domínguez-Fernández A. Acoustic emission analysis for the detection of appropriate cutting operations in honing processes. Mech Syst Signal Process 2018:99. https://doi.org/10.1016/j.ymssp.2017.06.039.
[7] Karpuschewski B, Welzel F, Risse K, Schorgel M. Reduction of friction in the cylinder running surface of internal combustion engines by the finishing process. Procedia CIRP 2016;vol. 45:87–90. https://doi.org/10.1016/j.procir.2016.02.338.
[8] Tripathi BN, Singh NK, Vates UK. Surface roughness influencing process parameters & modeling techniques for four stroke motor bike cylinder liners during honing: Review. Int J Mech Mechatron Eng 2015;15:106–12.
[9] Kadyrov RR, Charikov PN, Pryanichnikova VV. Honing process optimization algorithms. IOP Conf Ser Mater Sci Eng 2018:327. https://doi.org/10.1088/1757-899X/327/2/022052.
[10] Mezghani S, Demirci I, Yousfi M, El Mansori M. Running-in wear modeling of honed surface for combustion engine cylinderliners. Wear 2013;302:1360–9. https://doi.org/10.1016/j.wear.2013.01.026.
[11] Vrac D.S. , Sidjanin L.P. , Kovac P.P. , Balos S.S., 2013, The influence of honing process parameters on surface quality, productivity, cutting angle and coefficients of friction. ⟨Http://DxDoiOrg/101108/00368791211208679⟩.
[12] Szabo O. Examination of material removal process in honing: EBSCOhost. Acta Tech Corviniensis-Bull Eng 2014;7:35–8.
[13] Cabanettes F, Dimkovski Z, Rosén B-G. Roughness variations in cylinder liners induced by honing tools' wear. Precis Eng 2015;41:40–6. https://doi.org/10.1016/j.precisioneng.2015.01.004.
[14] Zhang X, Wang X, Wang D, Wang X, Yao Z, Xi L. Methodology to improve the cylindricity of engine cylinder bore by honing. ASME 2016 11th Int Manuf Sci Eng Conf MSEC 2016;2016:1. https://doi.org/10.1115/MSEC20168709.
[15] Xi C, Hu X, Zhang Z. Research for cylindricity prediction model of inner-hole honing. 2011 2nd Int Conf Mech Autom Control Eng MACE 2011 - Proc 2011:1506–9. https://doi.org/10.1109/MACE.2011.5987234.
[16] El Mansori M, Goeldel B, Sabri L. Performance impact of honing dynamics on surface finish of precoated cylinder bores. Surf Coat Technol 2013;215:334–9. https://doi.org/10.1016/j.surfcoat.2012.09.062.
[17] Takagi T, Sugeno M. Fuzzy identification of systems and its applications to modeling and control. IEEE Trans Syst Man Cyber 1985;SMC-15:116–32. https://doi.org/10.1109/TSMC.1985.6313399.
[18] Mamdani EH. Application of fuzzy algorithms for control of simple dynamic plant. Proc Inst Electr Eng 1974;121:1585–8. https://doi.org/10.1049/piee.1974.0328.
[19] Mamdani EH. Application of fuzzy logic to approximate reasoning using linguistic synthesis. IEEE Trans Comput 1977;C–26:1182–91. https://doi.org/10.1109/TC.1977.1674779.
[20] Buj-Corral I, Sánchez-Casas X, Luis-Pérez CJ. Analysis of am parameters on surface roughness obtained in pla parts printed with fff technology. Polym (Basel) 2021:13. https://doi.org/10.3390/polym13142384.
[21] Jang J-SR. ANFIS: adaptive-network-based fuzzy inference system. IEEE Trans Syst Man Cyber 1993;23:665–85. https://doi.org/10.1109/21.256541.
[22] Shihabudheen KV, Pillai GN. Recent advances in neuro-fuzzy system: A survey. Knowl-Based Syst 2018;152:136–62. https://doi.org/10.1016/j.knosys.2018.04.014.
[23] Pandiyan V, Shevchik S, Wasmer K, Castagne S, Tjahjowidodo T. Modelling and monitoring of abrasive finishing processes using artificial intelligence techniques:

A review. J Manuf Process 2020;57:114–35. https://doi.org/10.1016/j.jmapro.2020.06.013.
[24] Marani M, Zeinali M, Kouam J, Songmene V, Mechefske CK. Prediction of cutting tool wear during a turning process using artificial intelligence techniques. Int J Adv Manuf Technol 2020;111:505–15. https://doi.org/10.1007/s00170-020-06144-6.
[25] Abbas AT, Sharma N, Anwar S, Luqman M, Tomaz I, Hegab H. Multi-response optimization in high-speed machining of Ti-6Al-4V using TOPSIS-fuzzy integrated approach. Mater (Basel) 2020;13:1–14. https://doi.org/10.3390/ma13051104.
[26] Li W, Huang J, Fei J, Cao L, Yao C, Wang W. A statistical model for evaluating the tribological properties of paper-based friction materials. Tribol Int 2015;92:418–24. https://doi.org/10.1016/j.triboint.2015.07.025.
[27] Sudheer Kumar Varma N, Rajesh S, Sita Rama Raju K, Murali Krishnam Raju VV. Neural Network and Fuzzy Logic based prediction of Surface Roughness and MRR in Cylindrical Grinding Process. Mater Today Proc 2017;4:8134–41. https://doi.org/10.1016/j.matpr.2017.07.154.
[28] Feng C-X, Wang X, Yu Z. Neural networks modeling of honing surface roughness parameters defined by ISO 13565 (doi:DOI:) J Manuf Syst 2002;21:395–408. https://doi.org/10.1016/S0278-6125(02)80037-1.
[29] Buj-Corral I, Sivatte-Adroer M, Llanas-Parra X. Adaptive indirect neural network model for roughness in honing processes. Tribol Int 2020. https://doi.org/10.1016/j.triboint.2019.105891.
[30] Sharma N, Kumar S, Singh KK. Taguchi's DOE and artificial neural network analysis for the prediction of tribological performance of graphene nano-platelets filled glass fiber reinforced epoxy composites under the dry sliding condition. Tribol Int 2022;172:107580. https://doi.org/10.1016/j.triboint.2022.107580.
[31] Vališ D, Gajewski J, Žák L. Potential for using the ANN-FIS meta-model approach to assess levels of particulate contamination in oil used in mechanical systems. Tribol Int 2019;135:324–34. https://doi.org/10.1016/j.triboint.2019.03.012.
[32] ISO. ISO 6106.2013. Abrasive products — Checking the grain size of superabrasives 2013:9.
[33] ISO. ISO 6104:2005. Superabrasive products – Rotating grinding tools with diamond or cubic boron nitride – General survey, designation and multilingual nomenclature 2005:11.
[34] The MathWorks Inc. Fuzzy Logic ToolboxTMUser's Guide© Copyright 1995–2020 by The MathWorks, Inc. n.d.
[35] Versaci M, Calcagno S, Cacciola M, Morabito FC, Palamara IP. Standard Soft Computing Techniques for Characterization of Defects in Nondestructive Evaluation. Chapter 6. In: Burrascano P, Callegari S, Montisci A, Ricci M, Versaci M, editors. Ultrason. Nondestruct. Eval. Syst. Ind. Appl. Issues. Cham: Springer International Publishing; 2015. p. 175–99. https://doi.org/10.1007/978-3-319-10566-6. Chapter 6.
[36] Egaji OA, Griffiths A, Hasan MS, Yu HN. A comparison of Mamdani and Sugeno fuzzy based packet scheduler for MANET with a realistic wireless propagation model. Int J Autom Comput, 12; 2015. p. 1–13. https://doi.org/10.1007/s11633-014-0861-y.
[37] Luis Pérez CJ. A proposal of an adaptive neuro-fuzzy inference system for modeling experimental data in manufacturing engineering. Mathematics 2020:8. https://doi.org/10.3390/MATH8091390.
[38] Luis Pérez CJ. On the application of a design of experiments along with an anfis and a desirability function to model response variables. Symmetry (Basel) 2021:13. https://doi.org/10.3390/sym13050897.
[39] Derringer G, Suich R. Simultaneous optimization of several response variables. J Qual Technol 2018;12:214–9. https://doi.org/10.1080/00224065.1980.11980968.
[40] Buj-Corral I, Rodero-de-Lamo L, Marco-Almagro L. Optimization and sensitivity analysis of the cutting conditions in rough, semi-finish and finish honing. Mater (Basel) 2021;15:75. https://doi.org/10.3390/ma15010075.
[41] Sabri L, El Mansori M. Process variability in honing of cylinder liner with vitrified bonded diamond tools. Surf Coat Technol 2009;204:1046–50. https://doi.org/10.1016/j.surfcoat.2009.05.013.
[42] Buj-Corral I, Sivatte-Adroer M. Multi-objective optimization of material removal rate and tool wear in rough honing processes. Machines 2022:10. https://doi.org/10.3390/machines10020083.
[43] Bell SB, Maden H, Needham G. The influence of grit size and stone pressure on honing. Precis Eng 1981;3:47. https://doi.org/10.1016/0141-6359(81)90078-7.
[44] Lu Y, Li J, Liang R, Zhang Y, Luo M, Guo C. Investigation on the effect of honing parameters on cylindricity of engine cylinder liner. Int J Adv Manuf Technol 2020;111:3111–22. https://doi.org/10.1007/s00170-020-06321-7.